Available online at www.sciencedirect.com
ScienceDirect
Carbohydrate Research 342 (2007) 2793–2800
Carbohydrate RESEARCH

O-2 Substituted pyranosyl oxacarbenium ions are C-2–O-2 2-fold rotors with a strong *syn* preference

Andrei R. Ionescu,[a] Dennis M. Whitfield[b,*] and Marek Z. Zgierski[a]

[a]*Steacie Institute for Molecular Sciences, NRC Canada, 100 Sussex Drive, Ottawa, ON, Canada K1A 0R6*
[b]*Institute for Biological Sciences, NRC Canada, 100 Sussex Drive, Ottawa, ON, Canada K1A 0R6*

Received 9 July 2007; received in revised form 14 September 2007; accepted 20 September 2007
Available online 29 September 2007

Abstract—The substituent at O-2 of glycopyranosides is known to have a pronounced effect on both the formation and the cleavage of glycosides at C-1. This is primarily attributed to stereoelectronic effects on the formation and stability of the related glycopyranosyl oxacarbenium ions. Previous QM studies of 2-*O*-methyl substituted *manno* and *gluco* configured pyranosyl oxacarbenium ions found a preference for the methyl carbon to be *syn* to the CH-2 methine. This study examines the conformational preference of variously substituted O-2 tetrahydropyranosyl oxacarbenium ions and confirms this *syn* preference. Neutral analogues are shown to have the expected 3-fold rotation whereas the charged species exhibit 2-fold rotation about C-2–O-2. Natural bond order (NBO) calculations suggest that the dominant stabilizing interaction is a unimodal O-2 lone pair to C-1–O-5 π-bond hyperconjugative interaction. This *syn* conformational preference has important implications for mimics of glycopyranosyl oxacarbenium ion transition states. It also suggests a conformational based mechanism that can be exploited to tune the reactivity of glycopyranosyl donors in the glycosylation reaction.

Keywords: Glycosylation; Density functional theory; Quantum chemistry; Natural bond order analysis; Glycosyl processing enzymes

1. Introduction

Glycopyranosyl oxacarbenium ions are thought to be the intermediates or transition states in most of the reactions that form or degrade oligo- and polysaccharides.[1] These sugars include abundant polymers like cellulose, starch, and chitin as well as glycolipids and glycoproteins that cover cells. Furthermore, it is generally assumed that the conformation of such ions is an important determinant of their reactivity and is an important factor in the design of inhibitors for the enzymes that catalyze such reactions. Such inhibitors are already used as therapeutics for a variety of conditions such as diabetes, and as antiviral, antibacterial, and antifungal agents. However, experimental evidence for even the presence of such ions[2] let alone detailed conformational analysis is difficult to obtain and therefore electronic structure calculations are one of the few reliable methods to probe these questions. Considerations like these have led us to study these ions by quantum mechanical (QM) calculations.[3]

During our studies of the prototypic ions 2,3,4,6-tetra-*O*-methyl-D-mannopyranos-1-yl (**1**) and 2,3,4,6-tetra-*O*-methyl-D-glucopyranos-1-yl (**2**)[4] detailed conformational analysis led us to the conclusion that rotation about the C-2–O-2 bond is best described as a 2-fold rotor with the *syn* (CH-2–C-2–O-2–C(H_3)) torsion angle near 0° as the minimum and the *anti* conformation as the secondary minimum, see Figure 1.[5] The calculated energy difference was about 15 kJ mol^{-1} with the exact value depending on the method of calculation. Optimizations using either Hartree–Fock methods or density functional theory (DFT) led to the same geometrical conclusions. Natural bond order (NBO) analysis suggested that this *syn* conformer was stabilized by the hyperconjugation between one of the lone pairs on O-2 and the CH-2 antibonding orbital, which is further

* Corresponding author. E-mail: Dennis.Whitfield@nrc-cnrc.gc.ca

0008-6215/$ - see front matter
doi:10.1016/j.carres.2007.09.007

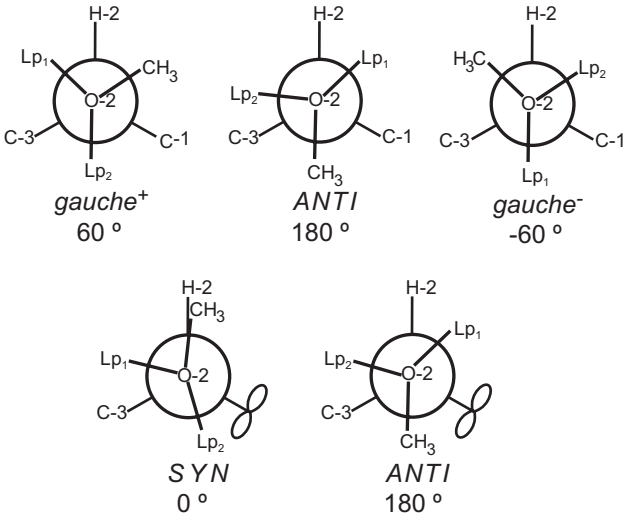

Figure 1. Newman projection along the C-2–O-2 bond showing the orientations of the electron pairs: (top) relative to C-1 corresponding to the neutral case, (bottom) relative to the p-type vacant orbital on C-1 corresponding to the cationic case; with values of the CH-2–C-2–O-2–C(H_3) dihedral angle shown.

conjugated to the vacant p-type orbital on C-1 of the cation. This analysis was, however, complicated by the large number of possible hyperconjugative interactions involving O-3, O-4, and O-6 in **1** and **2**. Therefore, we decided to study the C-2–O-2 rotamer populations by DFT calculations including NBO analysis of simpler model compounds. For comparative purposes we studied neutral compounds **3**–**6** and pyranosyl oxacarbenium ions **7**–**14** (see Scheme 1 for structures and numbering). Structures **3**, **5**, **7**, and **9** have C-2 equatorial methoxy substituents (using sugar numbering) whereas **4**, **6**, **8**, and **10** have epimeric axial methoxy substituents. Structures **5**, **6**, **9**, and **10** have an additional equatorial methoxy group at C-3. As well, a small selection of C-2 equatorial analogues **11**–**14** with prototypic substituents for common protecting groups were studied.

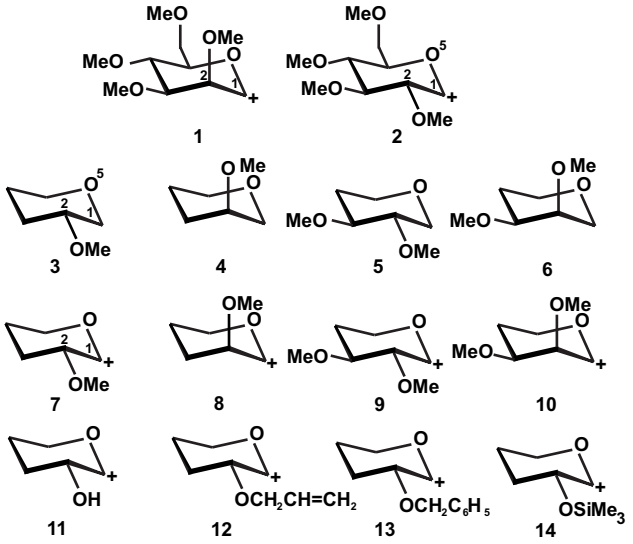

Scheme 1. Structures of neutral compounds and oxacarbenium ions from **1** to **14**. The sugar numbering is indicated on selected structures.

2. Results and discussion

For neutral compounds **3**–**6**, all the oxanol rings were found in the expected chair conformations ($^4C_1$ using sugar numbering). As well, the methoxy substituents at C-2 were calculated to have gauche conformations with the absolute values at the minima closer to 40° than 60°. This is consistent with the previous studies of *O*-methyl substituted sugars.[6] This rotational preference was further studied by performing rotational analysis with all degrees of freedom other than the C-2–O-2 torsion angle allowed to optimize. These rotations are plotted for equatorial substituted **3** and **5** in Figures 2a and 3a, and for axial substituted **4** and **6** in Figures 2c and 3c. In all cases, the rotation can be characterized as a 3-fold rotor with nearly equivalent *gauche*$^-$ and *gauche*$^+$ conformers as minima and a higher energy *anti* conformer as the third minimum. A small barrier is found at the *syn* conformation, with much higher barriers separating either *gauche* minimum from the *anti* minimum. Anderson et al. have presented evidence that the central 2-methoxy of all equatorial 1,2,3-trimethoxy substituted cyclohexanes also favor the *syn* conformer whereas the adjacent axial substituents (at 1 or 3) allow rotamers in between *syn* and *gauche* to be populated.[7] These authors ascribed this to subtle steric effects. Their results prompted the inclusion of the extra methoxy substituent in **5**, **6**, **9**, and **10**. The rotational preference about C-2–O-2H of D-glucose has been inferred from kinetic isotope effects and the preferences were suggested to arise from hyperconjugation between the O-2 lone pair (LP) and the CH-2 methine which is maximal for an *anti* relationship between these two entities.[8] Such an effect is a manifestation of the Bohlmann torsional effect.[9]

Typical structural and charge changes after ionization are compared for neutral **3** versus charged **7** in Table 1. All changes are in accord with an oxacarbenium ion structure for **7** with appreciable double bond character between C-1 and O-5 as well as considerable charge buildup on C-1 and O-5. For oxacarbenium ions **7**–**14**, the *syn* rotamers about C-2–O-2 were found to be the global minima with secondary *anti* minima. The energy difference between the minima depends on the substituent ranging from 0.6 for **14** to 14.3 kJ mol^{-1} for **9**, see Table 2. In all O-2 equatorial cases except **11** the C-2–O-2 bond length is longer for the *syn* conformer than the *anti* conformer by 0.01–0.03 Å. This bond lengthening trend follows the magnitude of the NBO energy

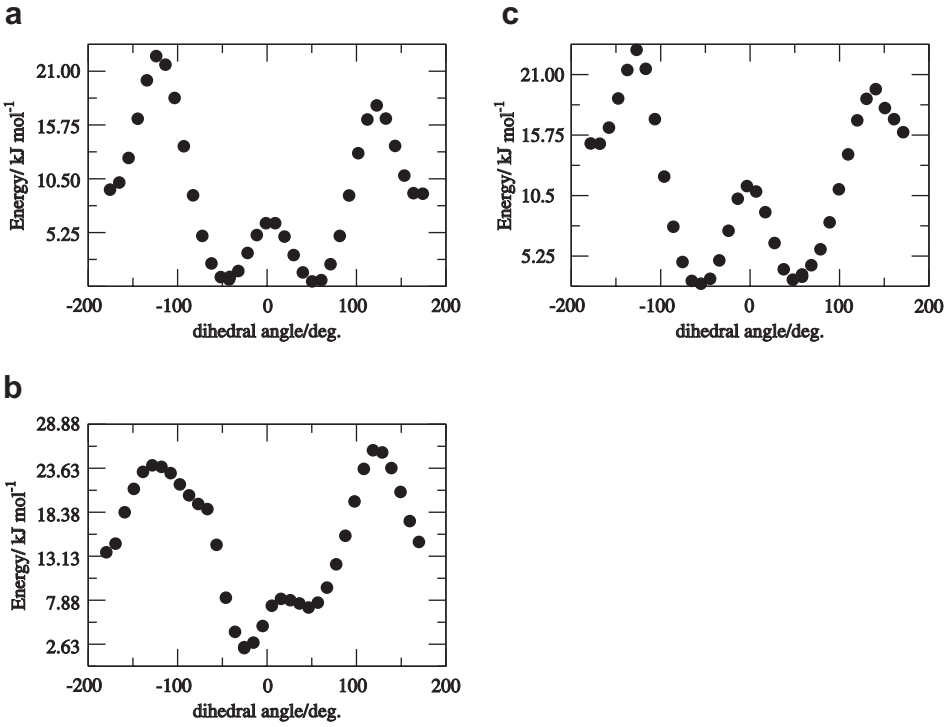

Figure 2. Potential energy curves for monomethoxy derivatives: equatorial (a) (**3**), (b) (**7**), and axial (c) (**4**). For axial (**8**) see Figure 4a. The absolute energy values of the minima are reported in the Supplementary data.

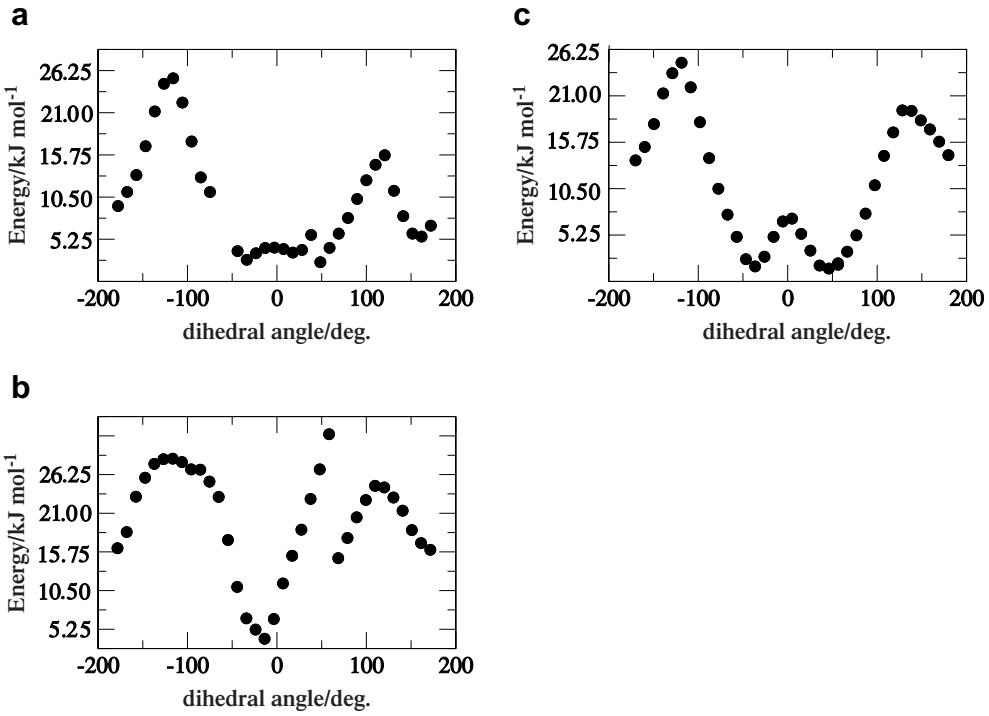

Figure 3. Potential energy curves for dimethoxy derivatives: equatorial (a) (**5**), (b) (**9**), and axial (c) (**6**). For axial (**10**) see Figure 4b. The absolute energy values of the minima are reported in the Supplementary data.

associated with the O-2 LP^2 to C-1–O5 π hyperconjugative interaction. This receiving orbital is the lowest unoccupied molecular orbital (LUMO) for glycopyranosyl oxacarbenium ions and therefore can be expected to

Table 1. Bond length (Å) and charge differences between **3** and **7**

Atom #	Delta *q*	Bond length	**3**	**7**
C-1	0.40	C-1–C-2	1.538	1.502
C-2	0.03	C-2–C-3	1.527	1.531
O(CH_3)	0.04	C-2–CH-2	1.101	1.102
CH_3	0.02	C-2–O(CH_3)	1.425	1.408
O-5	0.20	C-1–CH-1	1.093	1.093
		C-1–O-5	1.423	1.258

accept electron density.[5] The observed C-2–O-2 bond lengthening is consistent with this type of interaction. The larger trimethylsilyl (**14**), benzyl (**13**), and allyl (**12**) groups all have steric and electronic interactions with the tetrahydropyran ring which modifies the trends.

Rotational analysis for equatorial substituted ions **7** and **9** (see Figs. 2b and 3b) and for axially substituted **8** and **10** (Fig. 4a and b) suggests that the small *syn* barrier found in the neutral species is replaced by a stabilizing interaction. Inflections in the curves in Figures 2b and 4b suggest that the *gauche* energies are largely unchanged. These results corroborate the trends found with sugar derivatives **1** and **2**.

The same analysis for axial substituted ions **8** and **10** has an additional complication which is that once the C-2–O-2 bond is rotated away from the *syn* minimum in either direction, using the stepsize for **7** and **9**, the optimization procedure leads to ring inversion such that the O-2 substituent becomes equatorially oriented with ring conformations near $^1S_5$ or $B_{2,5}$. We had previously noted a similar effect with oxacarbenium ions like **1** and **2** where ions with O-2 sugar substituents prefer pseudo-equatorial orientations.[5] However, for *manno*-configured **1**, a stable *anti* conformer approximately 15 kJ mol^{-1} above the *syn* conformer was found. For neutral axially substituted **4** and **6** no ring inversion was observed. Repeating the rotation with a much smaller stepsize the C-2–O-2 rotational energy profiles still

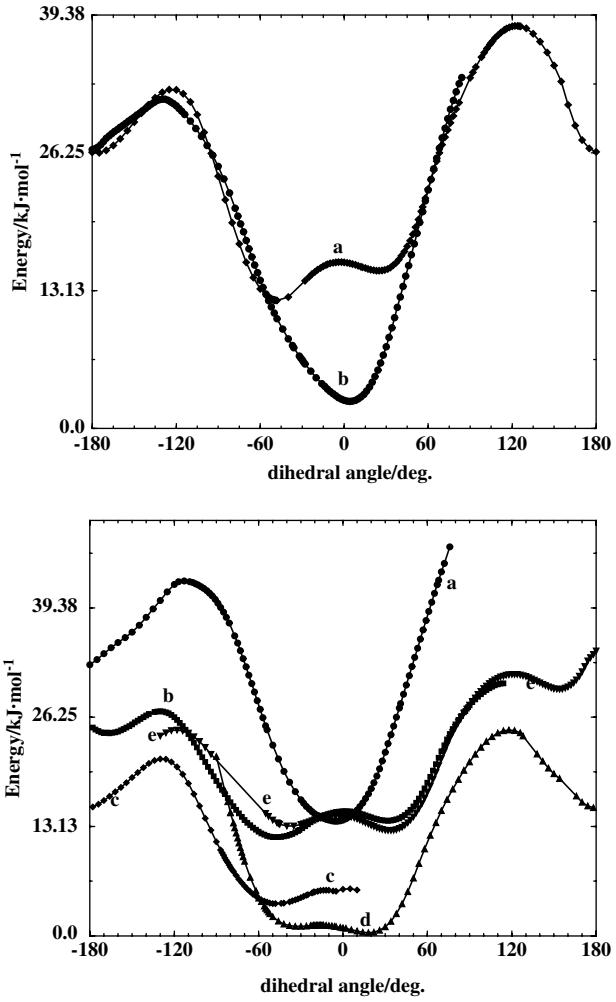

Figure 4. (a) Top potential energy curves for axial methoxy derivative **8**: curve a $^4H_3$, curve b $^1S_5$; (b) bottom potential energy curves for axial dimethoxy derivative **10**: curve a $^4H_3$, curve b $B_{2,5}$, curve c $^3H_4$, curve d $^3H_4$ different C-3–O-3 conformation from c, curve e $B_{2,5}$ different rotamers about C-3–O-3 from curve b. For (a) 0.0 = −384.487 a.u. and for (b) 0.0 = −499.936 a.u., 1 a.u. = 2625.4985 kJ mol^{-1}.

Table 2. Important structural, energetic and conformational data for oxacarbenium ions **7**–**14**

Comp.	*syn*/*anti* Δ*E*	CH-2–C-2–O-2–X dihedral (°)	C-2–O-2 bond length (Å)	O-2 LP–C-1–O-5 π bond NBO E	O-2 LP–C-2–H-2 σ^* Bond NBO E	Six-membered ring conformational descriptors
syn **7**	−10.5	−25.6	1.40659	−26.7	−13.4	0.936 $^4H_3$ 0.133 $^1S_3$ 0.003 $^{2,5}B$
anti **7**	—	−179.6	1.38783	−4.3	−13.3	0.961 $^4H_3$ 0.080 ^{2}E 0.019 $^4C_1$
syn **8**	−14.3	13.0	1.43306	−90.0	−10.1	0.764 ^4E 0.176 $^4C_1$ 0.016 ^2S_O
anti **8**	—	179.4	1.38349	<2.0	−13.9	0.846 $^1S_5$ 0.197 $^4C_1$ 0.080 $^{O,3}B$
syn **9**	−13.5	−24.3	1.41006	−35.2	−13.7	0.896 $^4H_3$ 0.157 $^1S_3$ 0.089 $B_{2,5}$
anti **9**		171.8	1.38249	−3.3	−12.8	0.953 $^4H_3$ 0.091 ^2E 0.041 $^4C_1$
syn **10**	−1.9	11.5	1.42361	−85.2	−11.4	0.759 ^4E 0.193 $^4C_1$ 0.044 ^2S_O
anti **10**	—	152.5	1.37251	−2.9	−9.0	0.098 $^4C_1$ 0.824 $B_{2,5}$ 0.157 $^1S_3$
syn **11**	−5.9	11.2	1.39468	−8.7	−14.4	1.023 $^4H_3$ 0.017 $^{2,5}B$ 0.001 $^4C_1$
anti **11**	—	167.3	1.39517	−9.4	−9.6	1.016 $^4H_3$ 0.035 $^{2,5}B$ 0.011 $^1S_3$
syn **12**	−12.6	−18.5	1.39976	−18.5	−15.6	0.972 $^4H_3$ 0.082 $^1S_3$ 0.002 $^{2,5}B$
anti **12**	—	−178.6	1.38925	−4.4	−13.1	0.962 $^4H_3$ 0.056 $^4C_1$ 0.022 $^{2,5}B$
syn **13**	−5.6	−21.6	1.39978	−15.7	−15.6	0.982 $^4H_3$ 0.075 $^1S_3$ 0.014 $^{2,5}B$
anti **13**	—	−173.4	1.39291	*	*	0.911 $^4H_3$ 0.112 $^4C_1$ 0.036 $^{2,5}B$
syn **14**	−0.6	−13.2	1.39477	−23.6	−25.1	0.936 $^4H_3$ 0.109 $^1S_3$ 0.054 $B_{2,5}$
anti **14**	—	−177.8	1.37867	−4.9	−20.6	0.868 $^4H_3$ 0.122 $^4C_1$ 0.000 $^{2,5}B$

* NBO Calculation did not converge.

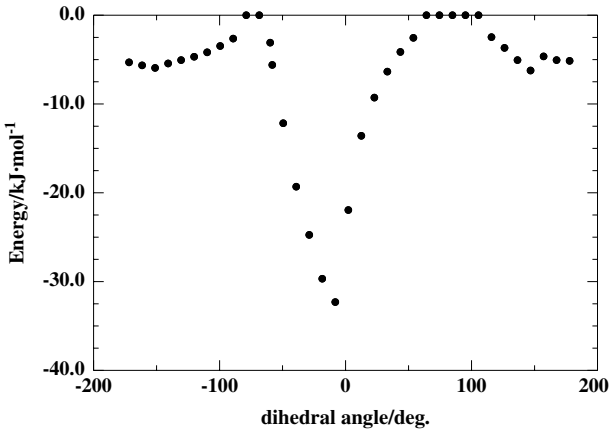

Figure 5. Hyperconjugation energy (from NBO calculation) between O-2 lone electron pair and C-1–O-5 π orbital plotted versus dihedral angle.

resemble those for **7** and **9** (see Fig. 4a for **8** and 4b for **10**). Notably, the 2-fold rotation profile with a *syn* minimum is found for all conformers. The conformers of **8** and **10** in Fig. 5a and b all differ by ring conformation or in the case of **10** by conformation about C-3–O-3. For **10**, curve a corresponds to the $^4H_3$ ring conformation and curve b to the $B_{2,5}$ conformation discussed above. Curves c and d have $^3H_4$ ring conformations but with different rotamers about C-3–O-3 and curve e is another $B_{2,5}$ ring conformation but with a different rotamers about C-3–O-3 from curve b. In spite of the apparent complication in defining the C-2–O-2 rotation profile created by these different conformers, these results support that the *syn* minima is a result of an interaction such as the hyperconjugative one we postulate below and is not related to the ring conformation or the C-3–O-3 side chain conformation. The O-3–CH_3 and the O-2–CH_3 do sterically interact as evidenced by the blips near CH-2–C-2–O-2–C(H_3) torsion angle near 50° in Figure 3a and b. The more pronounced effect for charged **9** and **10** (see Fig. 4) may be indicative of a steric buttressing effect reported for mannopyranosyl donors with larger than methyl protecting groups.[10]

Of the possible origins of this *gauche* to *syn* conformational change after ionization we first considered steric effects by analyzing the rotational curves for the neutral compounds **3**–**6**. In all these cases typical 3-fold rotors were found with a small barrier at the *syn* conformation, see Figure 3a and c.[11] To further test if this was perhaps a steric effect related to the different ring geometry $^4H_3$ in the ions (see Table 2) and $^4C_1$ in the neutrals, a rotational analysis for **3** with the ring fixed in the high energy $^4H_3$ conformation was made (not shown). It also revealed a 3-fold rotational dependence similar to **3** in its minimum energy $^4C_1$ ring conformation. A similar study aimed at assessing the influence of adjacent sp^2 hybridization with 3-methoxycyclohexene also found a 3-fold rotational dependence (not shown). Together, these results disfavor a steric explanation. Possible energetic explanations were then assessed by performing NBO analysis. These results provided a possible explanation for the 3-fold to 2-fold rotor change after ionization. As shown for ion **7** in Fig. 5, one NBO orbital has

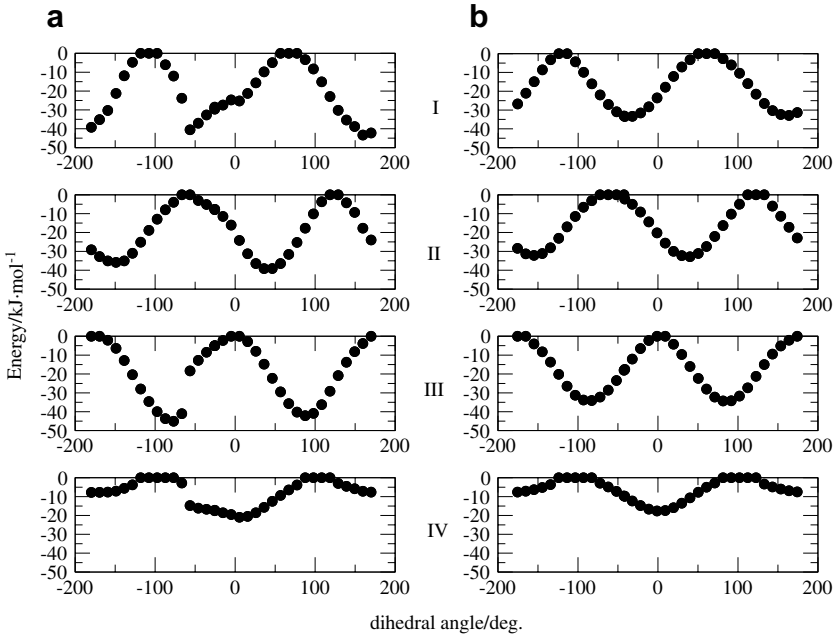

Figure 6. Hyperconjugation energy curves (from NBO calculations) between O-2–LP^2 to C-1–C-2 (I), C-2–C-3 (II), C-2–H-2 (III) and O-2–LP^1 to C-2–H-2 (IV) for (a) (**7**) and (b) (**3**).

a highly stabilizing interaction between the π-type lone pair on oxygen, LP^2, and the C-1–O-5 π-bond with a unimodal angular dependence with a maximum near CH-2–C-2–O-2–C(H_3) = 0°. As reported in Table 2, this interaction is larger for all *syn* conformers studied here except in the case of hydroxy **11**. The other lone pair does not interact with this orbital above the threshold value (0.5 kcal mol^{-1} = 2.092 kJ mol^{-1}). Note that the absolute energies from NBO analyses are not reliable but such values do provide a numeric method for assessing trends like the angular dependence found here.

Figure 6a shows some of the other NBO interactions for ion **7** that could also be significant such as the one associated with the Bohlmann effect, that is, O-2 LP^2 to CH-2 σ^* (III in Fig. 6a) as well as the O-2 LP^2 to the C-1–C-2 (I in Fig. 6a) and C-2–C-3 σ^* (II in Fig. 6a) orbitals. These same four interactions are shown in Figure 6b for neutral **3**. For **3**, the interactions I to III are all of similar magnitude and the overall rotational energy approximately tracks with these interactions. As well, the curves are all highly symmetric whereas for **7** the same interaction curves show asymmetry as could be expected. The combination of all these interactions will of course contribute to the overall rotational energy. Also shown in Fig. 6a is the interaction of O-2 LP^1 with the CH-2 σ^* (IV in Fig. 6a) and this interaction stabilizes near 0°. A similar trend for **1** and **2** was the basis of our previous provisional hypothesis for *syn* stabilization, but the much larger magnitude of the effect shown for **7** in Figure 5 provides a more compelling hypothesis.

To further corroborate these findings, the *syn*/*anti* energy difference for a number of oxacarbenium ion analogues of **7** with a small selection of prototypic hydroxyl protecting groups was calculated, **11**–**14**. These groups were proton (**11**), that is, the parent hydroxyl, allyl (**12**), benzyl (**13**), and trimethylsilyl (**14**). The special case of acyl protecting groups will be considered in a separate communication because these groups are capable of neighboring group participation.[12] In all cases studied here the *syn* conformer is lower in energy and NBO analysis finds the same stabilizing interaction, see Table 2. The parent hydroxyl compound **11** is anomalous and this result suggests an important difference between chemical glycosylation reactions with protecting groups and reactions of the 'free' sugars such as enzyme catalyzed reactions. The *syn* conformer for **11** is 5.9 kJ mol^{-1} more stable than the *anti* one, which is large enough to have an impact on reactivity. The *syn*/*anti* energy difference for the $^5S_1$ ring conformer of 3,4,6-tri-*O*-methyl-D-glucopyranosyl analogue of **2** is 3.1 kJ mol^{-1} favoring *syn* (*syn* C-2–O-2 −6.7°, *anti* 167.0°).

A previous QM study of **14** and **7** only presented data for the *anti* conformation suggesting that the *syn* preference is generally not well recognized.[13] The small energy difference for the TMS derivative **14** might be indicative of a steric effect counteracting the electronic effect.

3. Conclusions

This study provides evidence for a change from 3-fold rotation to 2-fold rotation for substituents adjacent to the developing positive charge in oxacarbenium ions. It is well known that the substituent at O-2 affects the reactivity of glycosyl donors in chemical glycosylation reactions.[14] A general trend of electron donating being activating and electron withdrawing being deactivating is well recognized and along with a number of related strategies forms the basis of one-pot synthesis and other reactivity-based synthetic methods.[15] The magnitude of the *syn*/*anti* difference observed here in some cases >10 kJ mol^{-1} is sufficient to account for these reactivity differences. Clearly this is not the only factor,[16] but it points to a conformational strategy that could be used to tune reactivity differences. That is, for otherwise similarly protected donors except for one whose ground state conformation is *anti* and one which is *syn*, the *syn* biased donor should be activated. It is a challenge to synthetic chemists to devise such a donor. One plausible strategy to such compounds is to replace the O-2 methyl group with a non-participating chiral protecting group.[17]

Similarly it seems probable to the authors that Nature would take advantage of this energy difference as one of the factors controlling reactivity in the numerous classes of glycosyl processing enzymes (GPE's) that are postulated to have oxacarbenium ion transition states or intermediates. In fact, it is well established that the electronic character of the substituent at O-2 can have a pronounced effect on the reactivity of GPE's.[18] This conformational property identified in this communication would suggest that hydrogen-bonding partners for the O-2 hydroxyl should be positioned *syn* or *anti* to CH-2 at the transition state for maximal effect. That is, *syn* if OH-2 is acting as a proton donor or *anti* if O-2 is acting as a proton acceptor. The former case mimics an electron withdrawing group and the latter case an electron donating group. This may be testable for enzymes whose transition states are relatively well known structurally.[19] For example, the class 1 α-mannosidase involved in N-glycan processing has a Ca^{+2} ion bound to O-2 and so with reasonable confidence the conformation about C-2–O-2 can be assigned as *syn* in a complex with a nonhydrolysable substrate.[20] Furthermore, transition state mimics that incorporate this *syn* O-2 design feature could be synthesized and tested.

4. Computational methods

The DFT calculations were carried out with the Amsterdam Density Functional (ADF) program system, ADF2005.[21] The atomic orbitals were described as an uncontracted triple-ζ Slater function basis set with a

single-ζ polarization function on all atoms which were taken from the ADF library (TPZ). The 1s electrons on carbon and oxygen were assigned to the core and treated by the frozen core approximation. A set of s, p, d, f, and g Slater functions centered on all nuclei were used to fit the electron density, and to evaluate the Coulomb and exchange potentials accurately in each SCF cycle. The local part of the V_{xc} potential (LDA) was described using the VWN parameterization,[22] in combination with the gradient corrected (CGA) Becke's functional[23] for the exchange and Perdew's function for correlation (BP86).[24] The CGA approach was applied self-consistently in geometry optimizations. Second derivatives were evaluated numerically by a two-point formula. The COSMO solvation parameters were dielectric constant $\varepsilon = 9.03$, ball radius = 2.4 Å, with atomic radii of C = 1.7, O = 1.4, and H = 1.2 Å.

Natural bond order (NBO) analysis was performed for all species to search for possible hyperconjugative interactions that might explain the 2- versus 3-fold rotation difference. NBO analysis is a method to separate localized energies, E(Lewis), from delocalization energies, E(Non-Lewis). The NBO analysis was performed through the inclusion of population keyword in GAUSSIAN 98[25] (B3LYP/6-311+G** basis set) using the NBO 3.1 program.[26] The filled NBOs of the natural Lewis structure describe covalency effects. The general transformation of canonical delocalized Hartree–Fock MOs to localized hybrid orbitals (NBOs) also leads to orbitals that are unoccupied in the formal Lewis structure.[27] The interactions between filled (donor) and unfilled (acceptor) orbitals represent the deviation of the molecule from the Lewis structure and can be used as a measure of delocalization.[28] The energy associated with the antibond orbitals can be numerically assessed by the deletion of these orbitals from the basis set and recalculation of the total energy.

Acknowledgments

This work was partly supported by the HPC multi scale modeling initiative of the NRC. The authors thank the NRC computer support group (IMSB) for ongoing assistance.

Supplementary data

Supplementary data associated with this article can be found, in the online version, at doi:10.1016/j.carres.2007.09.007.

References

1. Jung, K. H.; Schmidt, R. R. In *Carbohydrate Based Drug Discovery*; Wong, C. H., Ed.; Wiley VCH: Weinheim, 2002; Vol. 1, pp 609–660.
2. (a) Suzuki, S. S.; Matsumoto, K.; Kawamura, K.; Suga, S.; Yoshida, J.-I. *Org. Lett.* **2004**, *6*, 3755–3758; (b) Boebel, T. A.; Gin, D. Y. *J. Org. Chem.* **2005**, *70*, 5818–5826.
3. Nukada, T.; Bérces, A.; Whitfield, D. M. *Carbohydr. Res.* **2002**, *337*, 765–774.
4. Nukada, T.; Bérces, A.; Wang, L. J.; Zgierski, M. Z.; Whitfield, D. M. *Carbohydr. Res.* **2005**, *340*, 841–852.
5. Ionescu, A.; Wang, L.-J.; Zgierski, M. Z.; Nukada, T.; Whitfield, D. M. In *NMR Spectroscopy and Modeling of Carbohydrates*; Vliegenhart, H., Woods, R. J., Eds.; ACS Symposium Series 930; Oxford University Press, 2006; pp 302–319.
6. (a) Mendonca, A.; Johnson, G. P.; French, A. D.; Laine, R. A. *J. Phys. Chem. A* **2002**, *106*, 4115–4124; (b) Anderson, J. E.; Ijeh, A. I. *J. Chem. Soc., Perkin Trans. 2* **1994**, 1965–1967.
7. González-Outeirino, J.; Nasser, R.; Anderson, J. E. *J. Org. Chem.* **2005**, *70*, 2486–2493.
8. Lewis, B. E.; Schramm, V. L. *J. Am. Chem. Soc.* **2001**, *123*, 1327–1336.
9. Lii, J.-H.; Chen, K.-H.; Allinger, N. L. *J. Phys. Chem. A* **2004**, *108*, 3006–3015.
10. (a) Crich, D.; Dudkin, V. *Tetrahedron Lett.* **2000**, *41*, 5643–5646; (b) Crich, D.; Jayalath, P. *Org. Lett.* **2005**, *7*, 2277–2280; (c) Crich, D.; Jayalath, P.; Hutton, T. K. *J. Org. Chem.* **2006**, *71*, 3064–3070.
11. Tvaroŝka, I.; Carver, J. P. *J. Mol. Struct. (Theochem)* **1997**, *395*(396), 1–13.
12. Whitfield, D. M.; Nukada, T. *Carbohydr. Res.* **2007**, *342*, 1291–1304.
13. Denekamp, C.; Sandlers, Y. *J. Mass Spectrom.* **2005**, *40*, 1055–1063.
14. (a) Fraser-Reid, B.; Wu, Z.; Andrews, C. W.; Skowronski, E. *J. Am. Chem. Soc.* **1991**, *113*, 1434–1435; (b) Paulsen, H. *Adv. Carbohydr. Chem. Biochem.* **1971**, *26*, 127–195; (c) Demchenko, A. V. *Curr. Org. Chem.* **2003**, *7*, 35–79.
15. (a) Fraser-Reid, B.; Merritt, J. R.; Handlon, A. L.; Andrews, C. W. *Pure Appl. Chem.* **1993**, *65*, 779–786; (b) Zhang, Z.; Ollman, I. R.; Ye, X.-S.; Wishnat, R.; Baasov, T.; Wong, C.-H. *J. Am. Chem. Soc.* **1999**, *121*, 734–753; (c) Douglas, N. L.; Ley, S. V.; Lucking, U.; Warriner, S. L. *J. Chem. Soc., Perkin Trans. 1* **1998**, 51–58; (d) Tanaka, H.; Matoba, N.; Tsukamoto, H.; Takimoto, H.; Yamada, H.; Takahashi, T. *Synlett* **2005**, 824–828; (e) Codée, J. D. C.; Litjens, R. E. J. N.; van den Bos, L. J.; Overkleeft, H. S.; van der Marel, G. A. *Chem. Soc. Rev.* **2005**, *34*, 769–782; (f) Huang, X.; Huang, L.; Wang, H.; Ye, X.-S. *Angew. Chem., Int. Ed.* **2001**, *116*, 5221–5224.
16. Kamat, M. N.; Demchenko, A. V. *Org. Lett.* **2005**, *7*, 3215–3218.
17. (a) Kim, J.-H.; Yang, H.; Park, J.; Boons, G.-J. *J. Am. Chem. Soc.* **2005**, *127*, 12090–12097; (b) Kim, J.-W.; Yang, H.; Boons, G.-J. *Angew. Chem., Int. Ed.* **2005**, *44*, 947–949; (c) Kim, J.-W.; Yang, H.; Khot, V.; Whitfield, D. M.; Boons, G.-J. *Eur. J. Org. Chem.* **2006**, 5007–5028.
18. (a) Namchuk, M. N.; McCarter, J. D.; Becalski, A.; Andrews, T.; Withers, S. G. *J. Am. Chem. Soc.* **2000**, *122*, 1270–1277; (b) Richard, J. P.; Mccall, D. A.; Heo, C. K.; Toteva, M. M. *Biochem.* **2005**, *44*, 11872–11881; (c) Terinek, M.; Vasella, A. *Helv. Chim. Acta* **2004**, *87*, 3035–3049.
19. Schramm, V. L. *Curr. Opin. Struct. Biol.* **2005**, *15*, 604–613.
20. Karaveg, K.; Siriwardena, A.; Tempel, W.; Liu, Z. J.; Glushka, J.; Wang, B. C.; Moremen, K. W. *J. Biol. Chem.* **2005**, *280*, 16197–16207.

21. (a) Baerends, E. J.; Ellis, D. E.; Ros, P. *Chem. Phys.* **1973**, *2*, 41–51; (b) te Velde, G.; Baerends, E. J. *J. Comput. Phys.* **1992**, *99*, 84–98; (c) Fonseca Guerra, C.; Snijders, J. G.; te Velde, G.; Baerends, E. J. *Theor. Chim. Acta* **1998**, *99*, 391–403; (d) Versiuis, L.; Ziegler, T. *J. Chem. Phys.* **1988**, *88*, 322–328; (e) Fan, L.; Ziegler, T. *J. Chem. Phys.* **1992**, *96*, 9005–9012.
22. Vosko, S. H.; Wilk, L.; Nusair, M. *Can. J. Phys.* **1980**, *58*, 1200–1211.
23. Becke, A. D. *Phys. Rev. A* **1988**, *38*, 3098–3100.
24. Perdew, J. P. *Phys. Rev. B* **1986**, *34*, 7506–7516.
25. Frisch, M. J.; Trucks, G. W.; Schlegel, H. B.; Scuseria, G. E.; Robb, M. A.; Cheeseman, J. R.; Zakrzewski, V. G.; Montgomery, J. A., Jr.; Stratmann, R. E.; Burant, J. C.; Dapprich, S.; Millam, J. M.; Daniels, A. D.; Kudin, K. N.; Strain, M. C.; Farkas, O.; Tomasi, J.; Barone, V.; Cossi, M.; Cammi, R.; Mennucci, B.; Pomelli, C.; Adamo, C.; Clifford, S.; Ochterski, J.; Petersson, G. A.; Ayala, P. Y.; Cui, Q.; Morokuma, K.; Rega, N.; Salvador, P.; Dannenberg, J. J.; Malick, D. K.; Rabuck, A. D.; Raghavachari, K.; Foresman, J. B.; Cioslowski, J.; Ortiz, J. V.; Baboul, A. G.; Stefanov, B. B.; Liu, G.; Liashenko, A.; Piskorz, P.; Komaromi, I.; Gomperts, R.; Martin, R. L.; Fox, D. J.; Keith, T.; Al-Laham, M. A.; Peng, C. Y.; Nanayakkara, A.; Challacombe, M.; Gill, P. M. W.; Johnson, B.; Chen, W.; Wong, M. W.; Andres, J. L.; Gonzalez, C.; Head-Gordon, M.; Replogle, E. S.; Pople, J. A. GAUSSIAN *98*; Gaussian: Pittsburgh, PA, 2002.
26. Glendening, E. D.; Reed, A. E.; Carpenter, J. E.; Weinhold, F. NBO Version 3.1.
27. Foster, J. P.; Weinhold, F. *J. Am. Chem. Soc.* **1980**, *102*, 7211–7218.
28. (a) Reed, A. E.; Weinhold, F. *J. Chem. Phys.* **1983**, *78*, 4066–4073; (b) Reed, A. E.; Weinstock, R. B.; Weinhold, F. *J. Chem. Phys.* **1985**, *83*, 735–746.